Published in final edited form as:
J Pathol. 2009 October ; 219(2): 163–172. doi:10.1002/path.2578.

Transcription factor NFAT1 deficiency causes osteoarthritis through dysfunction of adult articular chondrocytes

J Wang[1,2], **BM Gardner**[1], **Q Lu**[1], **M Rodova**[1], **BG Woodbury**[1], **JG Yost**[1], **KF Roby**[3], **DM Pinson**[4], **O Tawfik**[4], and **HC Anderson**[4]

[1]Harrington Laboratory for Molecular Orthopedics, Department of Orthopedic Surgery, University of Kansas Medical Center, 3901 Rainbow Boulevard, Kansas City, Kansas 66160, USA.

[2]Department of Biochemistry and Molecular Biology, University of Kansas Medical Center, 3901 Rainbow Boulevard, Kansas City, Kansas 66160, USA.

[3]Cancer Center and Department of Anatomy and Cell Biology, University of Kansas Medical Center, 3901 Rainbow Boulevard, Kansas City, Kansas 66160, USA.

[4]Department of Pathology and Laboratory Medicine, University of Kansas Medical Center, 3901 Rainbow Boulevard, Kansas City, Kansas 66160, USA.

Abstract

Osteoarthritis (OA) is the most common form of joint disease in middle-aged and older people. Previous studies have shown that over expression of matrix-degrading proteinases and proinflammatory cytokines is associated with osteoarthritic cartilage degradation. However, it remains unclear which transcription factors regulate the expression of these cartilage-degrading molecules in articular chondrocytes. This study demonstrated that mice lacking Nfat1, a member of the nuclear factor of activated T-cells (NFAT) transcription factors, exhibited normal skeletal development but displayed loss of type-II collagen (collagen-2) and aggrecan with overexpression of specific matrix-degrading proteinases and proinflammatory cytokines in young adult articular cartilage of weight-bearing joints. These initial changes are followed by articular chondrocyte proliferation/clustering, progressive articular surface destruction, periarticular chondro-osteophyte formation, and exposure of thickened subchondral bone, all of which resemble human OA. Forced expression of *Nfat1* delivered with lentiviral vectors in cultured 3-month-old primary *Nfat1* knockout ($Nfat1^{-/-}$) articular chondrocytes partially or completely rescued the abnormal catabolic and anabolic activities of $Nfat1^{-/-}$ articular chondrocytes. These new findings revealed a previously unrecognized critical role of Nfat1 in maintaining the physiological function of differentiated adult articular chondrocytes through regulating the expression of specific matrix-degrading proteinases and proinflammatory cytokines. Nfat1 deficiency causes OA due to an imbalance between catabolic and anabolic activities of adult articular chondrocytes, leading to articular cartilage degradation and failed repair activities in and around articular cartilage. These results may provide new insights into the aetiology, pathogenesis and potential therapeutic strategies for osteoarthritis.

Keywords

osteoarthritis; animal models of human disease; NFAT1 transcription factor; gene-altered mice; proteinases; cytokines

Correspondence to J.W. (jwang@kumc.edu).

No conflicts of interest were declared.

No prior or duplicate publication or submission elsewhere of any part of the work has been included in the manuscript.

Introduction

OA is characterized histopathologically by progressive loss of articular cartilage, chondro-osteophyte formation, and thickening of subchondral bone [1–5]. Primary/idiopathic OA most commonly develops via unknown initial causes, while secondary OA develops after joint injuries/disorders with mechanical abnormalities [3–6]. Articular chondrocytes synthesize extracellular matrix containing collagen-2-rich collagenous networks that provide tensile strength and aggrecan-rich proteoglycans that resist compressive loads [7,8]. Osteoarthritic chondrocytes may display increased catabolic activity due to overexpression of matrix-degrading proteinases, abnormal anabolic activity, hypertrophic changes, and/or increased Wnt/β-catenin signaling depending on the stages of disease [7–14]. The molecular basis of these pathological cellular activities is poorly understood. Transcription factor Sox9 is critical for embryonic chondrogenesis [15], but is not the key regulator of collagen-2 expression in adult articular chondrocytes [10]. Therefore, key transcription factors regulating the metabolism of adult articular chondrocytes remain unidentified.

NFAT transcription factors were originally identified as regulators of gene transcription in response to T-cell receptor-mediated signals in lymphocytes. NFAT signaling also regulates bone formation and osteoclastic bone resorption [16–18]; however, the role of NFAT members in chondrogenesis has been controversial [19,20]. Nfat4 was reported to induce or enhance chondrogenesis [19]. In contrast, Nfatp (Nfat1/Nfatc2) was interpreted as a repressor/inhibitor of chondrogenesis and tumorigenesis based primarily on “neoplastic” cartilage proliferation in and around articular cartilage of adult *Nfat1*$^{-/-}$ mouse appendicular joints [20]. However, it remains unclear why Nfat1 deficiency-induced cartilage phenotype occurs in specific weight-bearing joints and whether loss of Nfat1 triggers any joint disease because neoplastic cartilaginous tumors rarely occur in articular cartilage. To address these questions, we recently examined the histopathological changes in the skeletal system of *Nfat1*-deficient mice with particular attention to the events occurring before 3 months and after 12 months of age, time points for which changes had not been presented in the previous report [20]. We found that proliferating and differentiating cartilage cells in *Nfat1*$^{-/-}$ mouse joints did not display diagnostic characteristics of neoplasia or cartilaginous tumors. However, these *Nfat1*$^{-/-}$ joints did show osteoarthritic changes, which resemble late-stage human OA [1,2,21]. The cellular and molecular mechanisms involved in the initiation and progression of Nfat1 deficiency-induced OA were elucidated in the present study.

Methods

Animals

The method for generation of *Nfat1*$^{-/-}$ mice was previously described [16]. All mice used in this study were bred and maintained in the Laboratory Animal Resources facility at the University of Kansas Medical Center (KUMC). All animal procedures were performed with the approval of the Institutional Animal Care and Use Committee at KUMC in compliance with all federal and state laws and regulations.

Histology, histochemistry, and immunohistochemistry

Mouse joint tissue samples were fixed in 2% paraformaldehyde, decalcified in 25% formic acid, and embedded in either paraffin or JB-4 plastic medium (Polysciences). Safranin-O and fast green stains were utilized to identify cartilage cells and matrices. 10% EDTA-decalcified tissue sections were used for immunohistochemical staining. To observe both immunoreaction and cellular morphology, some tissue sections were stained by the avidin-biotin peroxidase complex methods. AEC or DAB chromogen was used for color detection

[22]. Microscopic structure and cellular details of cartilaginous appendicular joints, cervical, thoracic, and lumbar vertebral joints (at least 3 segments per region), sternocostal joints, tail joints, and the xiphoid were examined at 1-day (newborn) and 1, 2, 3, 4, 6, 9, 12, 15, 18, and 24 months. At least five *Nfat1*$^{-/-}$ and WT mice were evaluated at each time point.

RNA isolation and gene expression analyses by quantitative real-time PCR (qPCR)

Since the early OA-like phenotype first occurs in the femoral heads and periarticular tissues of *Nfat1*$^{-/-}$ female mice and femoral head articular cartilage is thicker and more capable of being removed compared to other joints, female femoral head articular cartilage and periarticular tissues were collected for RNA isolation. Articular cartilage and periarticular tissue (synovium with underlying capsule and periosteum near articular cartilage) samples were dissected under a dissecting microscope to avoid contamination by surrounding tissues. Freshly dissected articular cartilage and periarticular tissues were collected in "RNA*later*" (Ambion) at 4°C, homogenized in TRIzol (Invitrogen), and treated with an RNeasy Mini Kit (Qiagen) and a DNA Digestion Kit (Ambion) to obtain purified RNA. One μg of total RNA and a "RETRO*Script*" kit (Ambion) were used for reverse transcription to yield cDNA. "Primer Express 3.0" software (Applied Biosystems) was used to design specific primers of target genes (Supplementary Table 1). qPCR reactions were performed in triplicate in 96-well plates using a 7500 Real-Time PCR system (Applied Biosystems) with "SYBR Green" for detection per manufacturer's instructions. Primers for rodent *Gapdh* (glyceraldehyde-3-phosphate dehydrogenase, Applied Biosystems) were used as internal controls [22, 23].

Western blot

Total protein was isolated from the organic phase following RNA isolation from cells/tissues according to the manufacturer's instructions (Invitrogen). Small aliquots were applied to 4–15% gradient SDS-PAGE, then transferred to a Hybond-P polyvinylidene difluoride membrane (Amersham Biosciences). After transfer, the membranes were blocked using 5% dry milk in PBS with 0.3% Tween 20 and incubated with specific primary antibodies against collagen-2, aggrecan, and Nfat1. Horseradish peroxidase (HRP)-conjugated anti-mouse (for Nfat1), anti-goat (for collagen-2), and anti-rabbit (for aggrecan) IgG (Santa Cruz) was used as the secondary antibody, which was detected using chemiluminescent HRP substrate (Millipore).

Preparation of lentiviral construct for Nfat1 expression

A lentiviral construct for stable expression of constitutively active Nfat1 was generated using a pCDH-EF1-MCS-T2A-copGFP lentiviral vector (System Biosciences). Mouse *Nfat1* cDNA with multiple serine-to-alanine mutations in the Nfat1 regulatory domain, which render Nfat1 constitutively active, was obtained from Addgene (plasmid 11792). This cDNA was transferred into the unique *Xba* site of the lentivector. The final construct was verified by sequencing.

Cell culture and DNA transfection

Articular cartilage cells were isolated from femoral heads of 3-month-old WT and *Nfat1*$^{-/-}$ female mice using collagenase D (1.5 mg/ml, Roche) in DMEM at 37°C for 3–4 hours. Primary cells were plated at 2×10^5 cells per 23-mm culture well in DMEM supplemented with 2 mM L-glutamine, 10% heat-inactivated fetal calf serum, and 1% penicillin/streptomycin, then placed into a humidified incubator with 5% CO_2 at 37°C. At 70–80% confluence, the cultures were transduced with lentiviral particles for forced expression of target genes. All cultures were replenished with fresh media three times per week. Packaging plasmid psPAX2 (Addgene), envelope plasmid pMD2.G (Addgene), and 293T cells (ATCC) were used for the production of viral particles.

Cell proliferation and transformation assays

Cell proliferation was assessed by plating isolated articular chondrocytes (5,000 cells/well) in a 96-well plate. Cells were cultured in the same media and conditions as described above. Cell proliferation rate was determined at 24, 48, 72, and 96 hours after cell attachment by CellTiter 96 Aq_{ueous} One Solution Cell Proliferation Assay per manufacturer's instructions (Promega, G3582). Cell transformation was assessed by soft agar assay for colony formation to detect the ability of cells to grow in the absence of adhesion/anchorage as previously described [24].

Quantitative detection of apoptosis by flow cytometry

Apoptosis of articular chondrocytes was detected and quantified by TUNEL assay (Roche, 11684795910) in which fluorescein-dUTP was conjugated to double-stranded break ends of apoptotic DNA by terminal deoxy-transferase (TdT). Cells for detection of apoptosis and negative/positive controls were cultured as described above and trypsinized 2 days after cell attachment, then further prepared per manufacturer's instructions. Flow cytometry was performed using a BD FACS Calibur cytometer and Cellquest software. FITC (fluorescein isothiocyanate) was excited using a 488-nm laser and detected with a 530/30 bp filter.

Statistical analyses

Unless otherwise stated, statistical analyses were performed with the Student's *t*-test (two-tailed) and were represented as means ± s.d. from at least three independent experiments for each experimental condition. $P < 0.05$ was considered statistically significant.

Results

OA-like changes in weight-bearing appendicular joints of adult *Nfat1*-deficient mice

Histopathological studies of the skeletal system revealed no abnormalities in newborn and 1-month *Nfat1*$^{-/-}$ mice (data not shown). At 2 months of age, the young adult stage in mice [25], loss of safranin-O-stained proteoglycans (Figure 1A–C), collagen-2 (Figure 1D), and aggrecan (Figure 1E) was first observed in female *Nfat1*$^{-/-}$ femoral head articular cartilage. Cell proliferation assay showed no difference in the rate of cell proliferation between *Nfat1*$^{-/-}$ and WT articular chondrocytes at this time. At 3–4 months, focal loss of proteoglycans and articular surface roughening with early chondrocyte clustering were seen in *Nfat1*$^{-/-}$ articular cartilage (Figure 1F). *Nfat1*$^{-/-}$ knees, ankles, shoulders, and elbows began to show focal loss of proteoglycans in articular cartilage at this stage (data not shown).

Early degradation of articular cartilage was followed by reparative cellular activity in *Nfat1*$^{-/-}$ articular cartilage and subchondral bone. Focal chondrocyte proliferation with increased proteoglycan staining became evident in the upper-middle zones of *Nfat1*$^{-/-}$ articular cartilage after 4 months. Chondrocyte differentiation/hypertrophy occurred in the deep-calcified zones of *Nfat1*$^{-/-}$ articular cartilage (Figure 1G). Reparative proliferating articular chondrocytes later formed cell clusters, but failed to regenerate deteriorated articular cartilage. Mesenchymal cells derived from subchondral bone marrow cavities differentiated into chondrocytes which underwent hypertrophy and endochondral ossification, leading to thickening of subchondral bone (Figure 1G–I).

From 12 to 24 months, progressive loss of articular cartilage and formation of subchondral bone cysts (Figure 1J), exposure of thickened subchondral bone (eburnation) (Figure 1K), and narrowing of joint space (Figure 1L) became evident in weight-bearing joints *of* *Nfat1*$^{-/-}$ mice. These histopathological changes were similar to those seen in late-stage human OA [1, 2, 21]. The OA-like phenotypes of *Nfat1*$^{-/-}$ mice occurred earlier in females

than males. Abnormal cartilage formation or osteoarthritic changes were not observed in or around other cartilaginous tissues such as the vertebral joints, sternocostal joints, tail joints, and the xiphoid (data not shown). Similar, but less severe OA-like changes were seen in older heterozygous (*Nfat1*$^{+/-}$) mice after 12 months, suggesting that *Nfat1* gene dosage affects the time of onset and severity of OA (data not shown).

Reparative chondrocytic activity was also activated in *Nfat1*$^{-/-}$ periarticular tissues (synovium and periosteum near articular cartilage). At 3–4 months, mesenchymal progenitor cells in periarticular tissues proliferated and differentiated into chondrocytes forming chondrophytes (Figure 2A–C). These chondrophytes subsequently underwent endochondral ossification and formed chondro-osteophytes or osteophytes around the margins of deteriorated articular cartilage (Figure 2D–G). The abnormal chondrocyte proliferation/differentiation and subsequent osteophyte formation occurring in *Nfat1*$^{-/-}$ periarticular tissues appeared to be a secondary reparative reaction to the initial articular cartilage degradation that had occurred prior to the formation of periarticular chondrophytes.

To address whether neoplastic changes occurred in *Nfat1*$^{-/-}$ mouse joints, four pathologists examined tissue slides of these joints. They unanimously concluded that these proliferating/differentiating cartilage cells in and around articular cartilage of *Nfat1*$^{-/-}$ joints did not display diagnostic characteristics of neoplasia (Figure 2B,C,E–G). Although not specific markers for chondrosarcoma, *Mapk1* (mitogen-activated protein kinase-1) and *Mapk9* were reported to be expressed at higher levels in chondrosarcomas and lower levels in enchondromas, but not in normal cartilage [26]. Our qPCR analyses demonstrated no significant differences in *Mapk1* and *Mapk9* expression between *Nfat1*$^{-/-}$ and WT articular cartilage or periarticular tissues, while their expression was significantly higher in rat chondrosarcoma cells (Figure 2H,I), suggesting that *Nfat1*$^{-/-}$ articular/periarticular cartilage is neither chondrosarcoma nor enchondroma. Furthermore, colony formation, a feature of cell transformation, was not detected in *Nfat1*$^{-/-}$ chondrocytes by soft agar assay (data not shown). Flow cytometric analysis of *Nfat1*$^{-/-}$ and WT chondrocytes demonstrated significantly more apoptotic cells in *Nfat1*$^{-/-}$ (Figure 2J,K), which is characteristic of human osteoarthritic chondrocytes [3, 7].

Loss of Nfat1 leads to an imbalance between catabolic and anabolic activities of adult articular chondrocytes

To explore the molecular and cellular mechanisms for the development of Nfat1 deficiency-induced OA, we examined the effects of Nfat1 deficiency on the catabolic and anabolic activities of articular chondrocytes during the initiation stage of OA (2–4 months). Catabolic activity was represented by increased expression levels of cartilage-degrading proteinases including MMPs (matrix metalloproteinases) and ADAMTS (a disintegrin and metalloproteinase with thrombospondin motifs), [8,27–29] and proinflammatory cytokines [11,30]. Anabolic activity was indicated by the expression of chondrocyte marker genes in articular cartilage. qPCR analyses demonstrated that expression of *Mmp1a, Mmp13*, and *Adamts5*, but not *Mmp−3, −8, −9* or *Adamts4* (data not shown), was significantly increased, while *Timp1* (tissue inhibitor of metalloproteinase-1) expression was decreased in *Nfat1*$^{-/-}$ articular cartilage (Figure 3A). Immunohistochemistry using aggrecan neo G1 antibody, which detects the degraded aggrecan product, displayed increased aggrecan degradation in *Nfat1*$^{-/-}$ articular cartilage (Figure 3B). The data suggest that Mmp13 and Adamts5 likely play major roles in degrading cartilage matrix at the initiation stage of Nfat1 deficiency-induced OA.

The expression of chondrocyte marker genes *Acan* (encoding aggrecan), *Col2α1*, *Col9α1*, and *Col11α1* (encoding collagen−2, −9, and −11) was decreased, while *Col10a1* (a hypertrophic chondrocyte marker) was elevated and temporally associated with the up-

regulation of *Ctnnb1* (encoding β-catenin) in *Nfat1*$^{-/-}$ articular cartilage (Figure 3C,D). However, no significant difference in *Sox9* expression was detected between WT and *Nfat1*$^{-/-}$ articular cartilage (Figure 3E). Expression levels of proinflammatory cytokine genes for IL-1β, IL-6, IL-17α, and TNFα (tumor necrosis factor-α) were up-regulated to varying degrees at 2–4 months (Figure 3F). Immunohistochemistry demonstrated substantially more intense IL-1β staining in *Nfat1*$^{-/-}$ than in WT articular cartilage (Figure 3G). Genes for anti-inflammatory cytokines (IL−4, −10, and −13) displayed no significant changes in *Nfat1*$^{-/-}$ articular cartilage (data not shown).

Forced expression of *Nfat1* using lentiviral vectors in cultured 3-month-old primary *Nfat1*$^{-/-}$ articular chondrocytes partially or completely rescued the abnormal catabolic and anabolic activities of *Nfat1*$^{-/-}$ articular chondrocytes (Figure 4A–C). These results suggest that Nfat1 deficiency causes an imbalance between catabolic and anabolic activities of young adult articular chondrocytes favoring catabolism, leading to increased cartilage degradation and decreased anabolic metabolism of articular chondrocytes at the initiation stage of OA.

Differential expression of specific growth factors between *Nfat1*$^{-/-}$ articular cartilage and periarticular tissues is associated with OA-like cartilage phenotypes

To explore the mechanisms by which *Nfat1*$^{-/-}$ articular cartilage showed reduced expression of chondrocyte markers, whereas *Nfat1*$^{-/-}$ periarticular tissues displayed enhanced cartilage formation during the initiation stage of OA, we analyzed the expression levels of a large number of growth factors in both articular cartilage and periarticular tissues at 1–4 months. Insulin-like growth factor-1 (IGF-1), transforming growth factor-β (TGF-β), and bone morphogenetic proteins (BMPs) are known to induce chondrogenic differentiation and/or maintain the function of chondrocytes. TGF-β1 and BMPs may also potentiate osteophyte formation [31–33]. Our qPCR analyses demonstrated that expression of several *Bmps*, *Igf1*, and *Tgfb1-3* decreased at 2–4 months in *Nfat1*$^{-/-}$ articular cartilage (Figure 5A,B), while *Bmp2*, *Bmp13*, *Bmp14*, and *Tgfb1-2* were up-regulated after 2 months in *Nfat1*$^{-/-}$ periarticular tissues (Figure 5C,D). *Acan*, *Col2a1*, and *Col10a1* expression was normal at 1–2 months and elevated at 3 months, correlating with chondrocyte differentiation in *Nfat1*$^{-/-}$ periarticular tissues (Figure 5E).

Our findings suggest that reduced anabolic activity of articular chondrocytes correlates with decreased expression of specific BMPs, TGF-βs, and IGF1, while enhanced periarticular cartilage differentiation is associated with up-regulated expression of specific BMPs and TGF-βs in *Nfat1*$^{-/-}$ joints around 3 months of age.

Discussion

The present study has demonstrated that the phenotypes of *Nfat1*$^{-/-}$ mouse joints fit the diagnostic characteristics of osteoarthritis, rather than those of neoplastic transformation. Although the development of chondro-osteophytes is exuberant and almost tumor-like in some of the hip joints, malignant-looking cartilage/bone cells or diagnostic characteristics of benign cartilaginous tumors are not seen in or around *Nfat1*$^{-/-}$ mouse joints. Furthermore, quantitative flow cytometric analysis and soft agar assay demonstrate that *Nfat1*$^{-/-}$ chondrocytes do not present any survival advantage as seen in tumor cells. Instead, these cells display a significant increase in apoptosis, which is one of the characteristics of human osteoarthritic chondrocytes [3,7]. This is consistent with previous mutation analyses of the NFAT1 gene which concluded that NFAT1 is not a tumor suppressor in human cartilaginous tumors [34]. A previous study [20] interpreted the cartilage proliferation in *Nfat1*$^{-/-}$ hip joints as neoplastic transformation and NFAT1 as a repressor of chondrogenesis and tumorigenesis, and thus NFAT1 inhibitors were proposed as potential targets for the

treatment of arthritic cartilage lesions. Our new findings have revealed a better understanding of the function of NFAT1 in cartilage biology and pathology. Nfat1 deficiency causes dysfunction of articular chondrocytes and progressive loss of articular cartilage, and cartilage proliferation observed in *Nfat1*$^{-/-}$ joints appears to be a secondary reparative reaction. Thus, the potential targets for the treatment of OA should be NFAT1 and/or its activators/enhancers, not NFAT1 inhibitors. Nevertheless, the previous report [20] discovered the cartilage phenotype of *Nfat1*$^{-/-}$ mice, and this scientific contribution should be highly appreciated.

The results indicate that the morphological, cellular, and molecular biological changes in and around affected *Nfat1*$^{-/-}$ articular cartilage vary with the progression of OA. Early pathological changes such as loss of proteoglycans with essentially normal articular structure and variations in expression of proteinases and cytokines observed in this animal model may not be seen in human OA specimens, which are mostly harvested at the late-stage of disease. However, these early morphological and molecular biological alterations are important clues for exploring the mechanisms for the initiation of OA.

The initial loss of proteoglycans and collagen-2 in *Nfat1*$^{-/-}$ articular cartilage apparently triggers reparative cellular activity with increased expression of specific growth factors and cartilage differentiation in periarticular tissues favoring chondro-osteophyte formation. Reparative chondrocyte proliferation and differentiation are also observed in *Nfat1*$^{-/-}$ articular cartilage and subchondral trabecular bone. This is consistent with the repair process in human OA [3,6,35]. Therefore, it is not surprising that expression of collagen-2 and -10 were up-regulated in *Nfat1*$^{-/-}$ articular cartilage and periarticular tissues at later disease stages, as reported in a previous publication [20]. It is important to point out that collagen-10 is a marker of hypertrophic chondrocytes, which is normally expressed in replacement cartilage in the growth plate during endochondral ossification, and not in persistent cartilage such as articular cartilage. Chondrocyte hypertrophy with up-regulated expression of collagen-10 is also an important feature of human osteoarthritic cartilage [6,7,9,12]. Highly upregulated expression of collagen-10 in *Nfat1*$^{-/-}$ articular cartilage supports our diagnosis of OA in *Nfat1*$^{-/-}$ mouse joints. However, these reactions in and around affected *Nfat1*$^{-/-}$ articular cartilage fail to regenerate deteriorated articular surface because these cells are not permanent articular chondrocytes in nature. Mechanisms for Nfat1 deficiency-induced cartilage degradation and possible interactions between articular cartilage and surrounding tissues are summarized in Figure 6.

Our novel findings demonstrate for the first time that Nfat1 is a key transcription factor regulating the expression of specific cartilage-degrading proteinases and proinflammatory cytokines in adult articular chondrocytes. Nfat1 deficiency causes OA due to dysfunction of adult articular chondrocytes, leading to articular cartilage degradation and repair activities in and around articular cartilage. These results may provide new insights into the etiopathogenesis of primary OA. NFAT1 may prove to be a suitable target for the development of new drugs for the prevention and treatment of OA upon determining that NFAT1 deficiency is associated with the development of human OA.

Supplementary Material

Refer to Web version on PubMed Central for supplementary material.

Acknowledgments

We thank Krishnan Unni (Mayo Clinic, Rochester, USA) for expert pathological consultation, Laurie Glimcher (Harvard University School of Public Health, Boston, USA) for providing breeder pairs of Nfat1-deficient mice, Joyce Slusser (University of Kansas, Kansas City, USA) for flow cytometric analyses of chondrocyte apoptosis,

and Benoit de Crombrugghe (University of Texas M. D. Anderson Cancer Center, Houston, USA) for providing rat chondrosarcoma cells. We also thank Linda Sandell (Washington University, St. Louis, USA), Kenneth Brandt (Indiana University, Indianapolis, USA), Daniel Stechschulte (University of Kansas, Kansas City, USA), and Marc Asher (University of Kansas, Kansas City, USA) for thoughtful discussion and/or critical reading of this manuscript. This work was supported in part by US National Institutes of Health (NIH) grants AR052088, DE05262, P20 RR016443 from the COBRE, site license provided in part by NIH grant P20 RR16475 from the INBRE program of the National Center for Research Resources, and the Mary Alice & Paul R. Harrington Endowment.

References

1. Pritzker KP, Gay S, Jimenez SA, Ostergaard K, Pelletier JP, Revell PA, et al. Osteoarthritis cartilage histopathology: grading and staging. Osteoarthritis Cartilage. 2006; 14:13–29. [PubMed: 16242352]
2. Hough, AJ. Pathology of Osteoarthritis. In: Moskowitz, RW.; Altman, RD.; Hochberg, MC.; Buckwalter, JA.; Goldberg, VM., editors. Osteoarthritis: Diagnosis and Medical/Surgical Management. Philadelphia: Wolters Kluwer/Lippincott Williams & Wilkins; 2007. p. 51-72.
3. Poole, AR.; Guilak, F.; Abramson, SB. Etiopathogenesis of Osteoarthritis. In: Moskowitz, RW.; Altman, RD.; Hochberg, MC.; Buckwalter, JA.; Goldberg, VM., editors. Osteoarthritis: Diagnosis and Medical/Surgical Management. Philadelphia: Wolters Kluwer/Lippincott Williams & Wilkins; 2007. p. 27-49.
4. Burr DB. The importance of subchondral bone in the progression of osteoarthritis. J Rheumatol Suppl. 2004; 70:77–80. [PubMed: 15132360]
5. Buckwalter JA, Mankin HJ, Grodzinsky AJ. Articular cartilage and osteoarthritis. Instr Course Lect. 2005; 54:465–480. [PubMed: 15952258]
6. Goldring MB, Goldring SR. Osteoarthritis. J Cell Physiol. 2007; 213:626–634. [PubMed: 17786965]
7. Sandell, LJ.; Heinegard, D.; Hering, TM. Cell Biology, Biochemistry, and Molecular Biology of Articular Cartilage in Osteoarthritis. In: Moskowitz, RW.; Altman, RD.; Hochberg, MC.; Buckwalter, JA.; Goldberg, VM., editors. Osteoarthritis: Diagnosis and Medical/Surgical Management. 4th edn. Philadelphia: Wolters Kluwer/Lippincott Williams & Wilkins; 2007. p. 73-106.
8. Karsenty G. An aggrecanase and osteoarthritis. New England Journal of Medicine. 2005; 353:522–523. [PubMed: 16079379]
9. Kirsch T, Swoboda B, Nah H. Activation of annexin II and V expression, terminal differentiation, mineralization and apoptosis in human osteoarthritic cartilage. Osteoarthritis Cartilage. 2000; 8:294–302. [PubMed: 10903884]
10. Aigner T, Gebhard PM, Schmid E, Bau B, Harley V, Poschl E. SOX9 expression does not correlate with type II collagen expression in adult articular chondrocytes. Matrix Biology. 2003; 22:363–372. [PubMed: 12935820]
11. Goldring SR, Goldring MB. The role of cytokines in cartilage matrix degeneration in osteoarthritis. Clin Orthop Relat Res. 2004; 427 Suppl:S27–S36. [PubMed: 15480070]
12. Tchetina EV, Squires G, Poole AR. Increased type II collagen degradation and very early focal cartilage degeneration is associated with upregulation of chondrocyte differentiation related genes in early human articular cartilage lesions. J Rheumatol. 2005; 32:876–886. [PubMed: 15868625]
13. Zhu M, Tang D, Wu Q, Hao S, Chen M, Xie C, et al. Activation of beta-catenin signaling in articular chondrocytes leads to osteoarthritis-like phenotype in adult beta-catenin conditional activation mice. J Bone Miner Res. 2009; 24:12–21. [PubMed: 18767925]
14. Kawaguchi H. Regulation of osteoarthritis development by Wnt-beta-catenin signaling through the endochondral ossification process. J Bone Miner Res. 2009; 24:8–11. [PubMed: 19016582]
15. Bi W, Deng JM, Zhang Z, Behringer RR, de Crombrugghe B. Sox9 is required for cartilage formation. Nat Genet. 1999; 22:85–89. [PubMed: 10319868]
16. Hodge M, Ranger A, Charles de la Brousse F, Hoey T, Grusby M, Glimcher L. Hyperproliferation and dysregulation of IL-4 expression in NF-ATp-deficient mice. Immunity. 1996; 4:397–405. [PubMed: 8612134]

17. Koga T, Matsui Y, Asagiri M, Kodama T, de Crombrugghe B, Nakashima K, et al. NFAT and Osterix cooperatively regulate bone formation. Nature Medicine. 2005; 11:880–885.
18. Takayanagi H, Kim S, Koga T, Nishina H, Isshiki M, Yoshida H, et al. Induction and activation of the transcription factor NFATc1 (NFAT2) integrate RANKL signaling in terminal differentiation of osteoclasts. Dev Cell. 2002; 3:889–901. [PubMed: 12479813]
19. Tomita M, Reinhold M, Molkentin J, Naski M. Calcineurin and NFAT4 induce chondrogenesis. J Biol Chem. 2002; 277:42214–42218. [PubMed: 12239209]
20. Ranger AM, Gerstenfeld LC, Wang J, Kon T, Bae H, Gravallese EM, et al. The nuclear factor of activated T cells (NFAT) transcription factor NFATp (NFATc2) is a repressor of chondrogenesis. J Exp Med. 2000; 191:9–21. [PubMed: 10620601]
21. Bullough, PG. Orthopaedic Pathology. 4th edn. Edinburgh: Mosby; 2004. Arthritis; p. 239-284.
22. Wang J, Zhou HY, Salih E, Xu L, Wunderlich L, Gu X, et al. Site-specific in vivo calcification and osteogenesis stimulated by bone sialoprotein. Calcif Tissue Int. 2006; 79:179–189. [PubMed: 16969594]
23. Livak KJ, Schmittgen TD. Analysis of relative gene expression data using real-time quantitative PCR and the 2-ΔΔCt Method. Methods. 2001; 25:402–408. [PubMed: 11846609]
24. Banning A, Kipp A, Schmitmeier S, Lowinger M, Florian S, Krehl S, et al. Glutathione Peroxidase 2 Inhibits Cyclooxygenase-2-Mediated Migration and Invasion of HT-29 Adenocarcinoma Cells but Supports Their Growth as Tumors in Nude Mice. Cancer Res. 2008; 68:9746–9753. [PubMed: 19047153]
25. Jacoby, RO.; Fox, JG.; Davisson, M. Biology and Diseases of Mice. In: Fox, JG.; Anderson, LC.; Loew, FM.; Quimby, FW., editors. Laboratory Animal Medicine. 2nd edn. San Diego: Academic Press; 2002. p. 35-120.
26. Papachristou DJ, Papachristou GJ, Papaefthimiou OA, Agnantis NJ, Basdra EK, Papavassiliou AG. The MAPK-AP-1/-Runx2 signalling axes are implicated in chondrosarcoma pathobiology either independently or via up-regulation of VEGF. Histopathology. 2005; 47:565–574. [PubMed: 16324193]
27. Glasson SS, Askew R, Sheppard B, Carito B, Blanchet T, Ma HL, et al. Deletion of active ADAMTS5 prevents cartilage degradation in a murine model of osteoarthritis. Nature. 2005; 434:644–648. [PubMed: 15800624]
28. Stanton H, Rogerson FM, East CJ, Golub SB, Lawlor KE, Meeker CT, et al. ADAMTS5 is the major aggrecanase in mouse cartilage in vivo and in vitro. Nature. 2005; 434:648–652. [PubMed: 15800625]
29. Burrage P, Mix K, Brinckerhoff C. Matrix metalloproteinases: role in arthritis. Front Biosci. 2006; 11:529–543. [PubMed: 16146751]
30. van den Berg, WB.; van der Kraan, PM.; van Beuningen, HM. Synovial mediators of cartilage damage and repair in osteoarthritis. In: Brandt, KD.; Doherty, M.; Lohmander, LS., editors. Osteoarthritis. 2nd edn. Oxford: Oxford University Press; 2003. p. 147-155.
31. Mi Z, Ghivizzani SC, Lechman ER, Jaffurs D, Glorioso JC, Evans CH, et al. Adenovirus-mediated gene transfer of insulin-like growth factor 1 stimulates proteoglycan synthesis in rabbit joints. Arthritis & Rheumatism. 2000; 43:2563–2570. [PubMed: 11083281]
32. Scharstuhl A, Vitters EL, van der Kraan PM, van den Berg WB. Reduction of osteophyte formation and synovial thickening by adenoviral overexpression of transforming growth factor beta/bone morphogenetic protein inhibitors during experimental osteoarthritis. Arthritis & Rheumatism. 2003; 48:3442–3451. [PubMed: 14673995]
33. Shuler FD, Georgescu HI, Niyibizi C, Studer RK, Mi Z, Johnstone B, et al. Increased matrix synthesis following adenoviral transfer of a transforming growth factor beta1 gene into articular chondrocytes. Journal of Orthopaedic Research. 2000; 18:585–592. [PubMed: 11052495]
34. Aoyama T, Nagayama S, Okamoto T, Hosaka T, Nakamata T, Nishijo K, et al. Mutation analyses of the NFAT1 gene in chondrosarcomas and enchondromas. Cancer Lett. 2002; 186:49–57. [PubMed: 12183075]
35. Sandell LJ. Anabolic factors in degenerative joint disease. Curr Drug Targets. 2007; 8:359–365. [PubMed: 17305513]

36. Samuels J, Krasnokutsky S, Abramson SB. Osteoarthritis: a tale of three tissues. Bull NYU Hosp Jt Dis. 2008; 66:244–250. [PubMed: 18937640]

37. Brandt KD, Dieppe P, Radin EL. Etiopathogenesis of osteoarthritis. Rheum Dis Clin North Am. 2008; 34:531–559. [PubMed: 18687271]

38. Felson DT, Gale DR, Elon Gale M, Niu J, Hunter DJ, Goggins J, et al. Osteophytes and progression of knee osteoarthritis. Rheumatology. 2005; 44:100–104. [PubMed: 15381791]

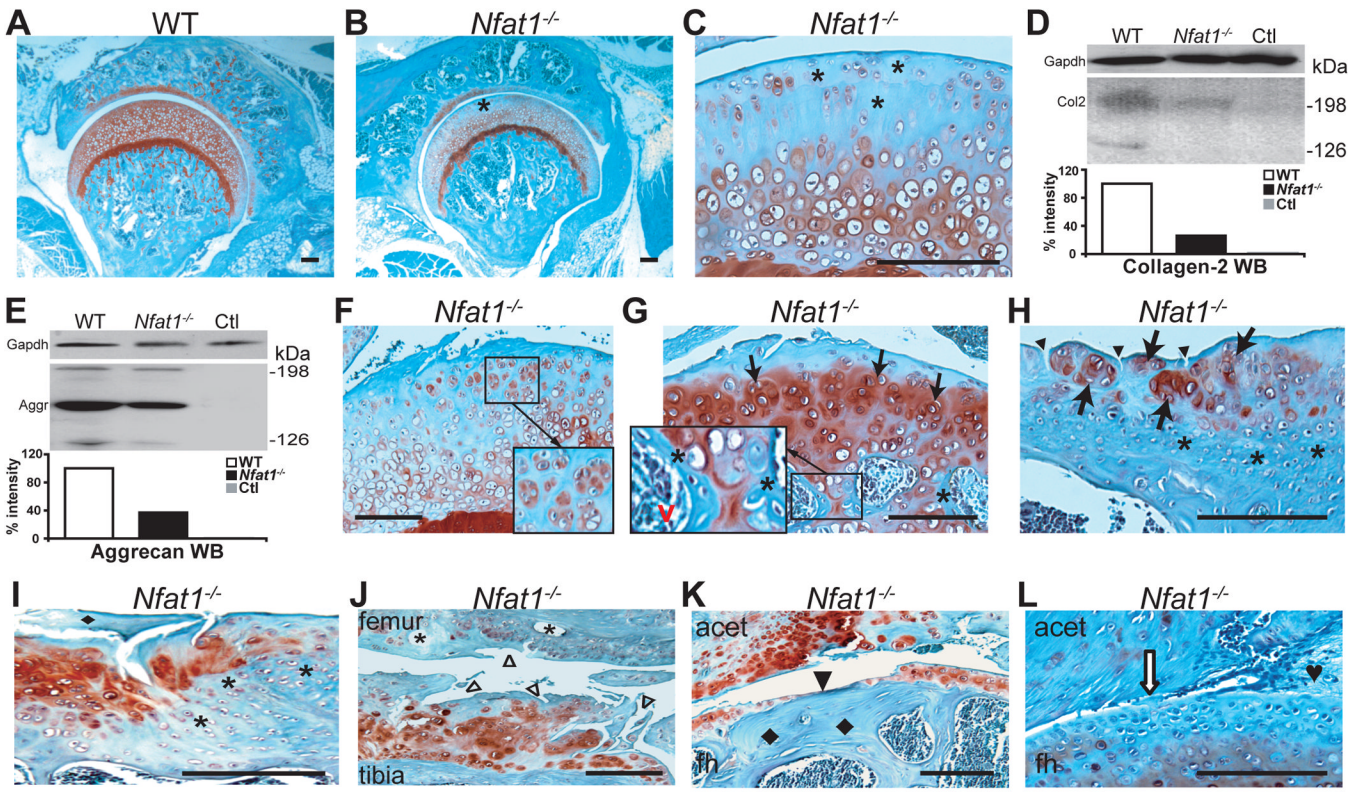

Figure 1.

Nfat1 deficiency causes OA-like changes in weight-bearing appendicular joints of adult mice. All photomicrographs are representative of at least 5 *Nfat1*$^{-/-}$ or WT mice per gender at each time point. Safranin-O and fast green staining and counterstained with hematoxylin. Scale bar = 200 μm. (**A**) A 2-month-old female WT mouse hip joint showing normal joint structure and articular surface with safranin-O staining (red) for proteoglycans throughout the entire articular cartilage. (**B**) At 2 months of age, a focal loss of safranin-O staining for proteoglycans is evident in the superficial/upper zone (*) of femoral head articular cartilage of a female *Nfat1*$^{-/-}$ mouse. Formation of abnormal periarticular cartilage is not evident at this stage. (**C**) Higher magnification of (B). (**D**) At 2 months, Western blot (WB) using a polyclonal antibody against human (cross-reacts with mouse) collagen-2 (Col2, Santa Cruz, sc-7764) with semi-quantitative measurements of band intensity reveals a loss of collagen-2 in female *Nfat1*$^{-/-}$ femoral heads. WB using Gapdh antibody (IMGENEX, IMG-3073) was used as a loading control. Ctl represents a negative control without using primary antibody. (**E**) At 2 months, a severe loss of aggrecan in female *Nfat1*$^{-/-}$ femoral heads was detected by WB using a polyclonal antibody against human (cross-reacts with mouse) aggrecan (Aggr, Santa Cruz, sc-25674) with semi-quantitative measurements of band intensity. (**F**) At 4 months, roughening of the articular surface, focal loss of proteoglycan staining, and early chondrocyte clustering (in magnified square) are seen in the upper-mid zones of articular cartilage of a female *Nfat1*$^{-/-}$ hip. (**G**) A 6-month *Nfat1*$^{-/-}$ hip joint shows roughening and discontinuity of articular surface, loss of safranin-O staining in the upper zone, chondrocyte clustering in the upper-mid zones (arrows), and increased safranin-O staining in mid-deep zones of femoral head articular cartilage. Endochondral ossification, including chondrocyte differentiation/hypertrophy, vascular invasion (red v), and new bone formation (*) on the surfaces of calcifying cartilage, is seen in subchondral bone (in magnified rectangle). (**H**) A 12-month *Nfat1*$^{-/-}$ shoulder (glenoid) shows chondrocyte clusters (arrows) with thickened subchondral bone (*) and vertical clefts in the superficial zone of articular cartilage

(arrowheads). (**I**) A 15-month *Nfat1*$^{-/-}$ humeral head displays a fragment of cartilage (♦) derived from deteriorated articular cartilage due to a combination of horizontal and vertical fissures/clefts. Increased proteoglycan staining (red) is evident in the areas adjacent to the fissures. Thickened subchondral bone (*) is clearly seen. (**J**) At 15 months, articular cartilage destruction with surface fibrillation (△) and subchondral bone cysts (*) are seen in an *Nfat1*$^{-/-}$ knee joint. (**K**) An 18-month *Nfat1*$^{-/-}$ hip shows thinning or complete loss of articular cartilage (eburnation) (arrowhead) with exposure of thickened subchondral bone (♦). acet, acetabulum; fh, femoral head. (**L**) An 18-month *Nfat1*$^{-/-}$ hip shows narrowing of joint space (open arrow) and fibrous joint fusion (♥).

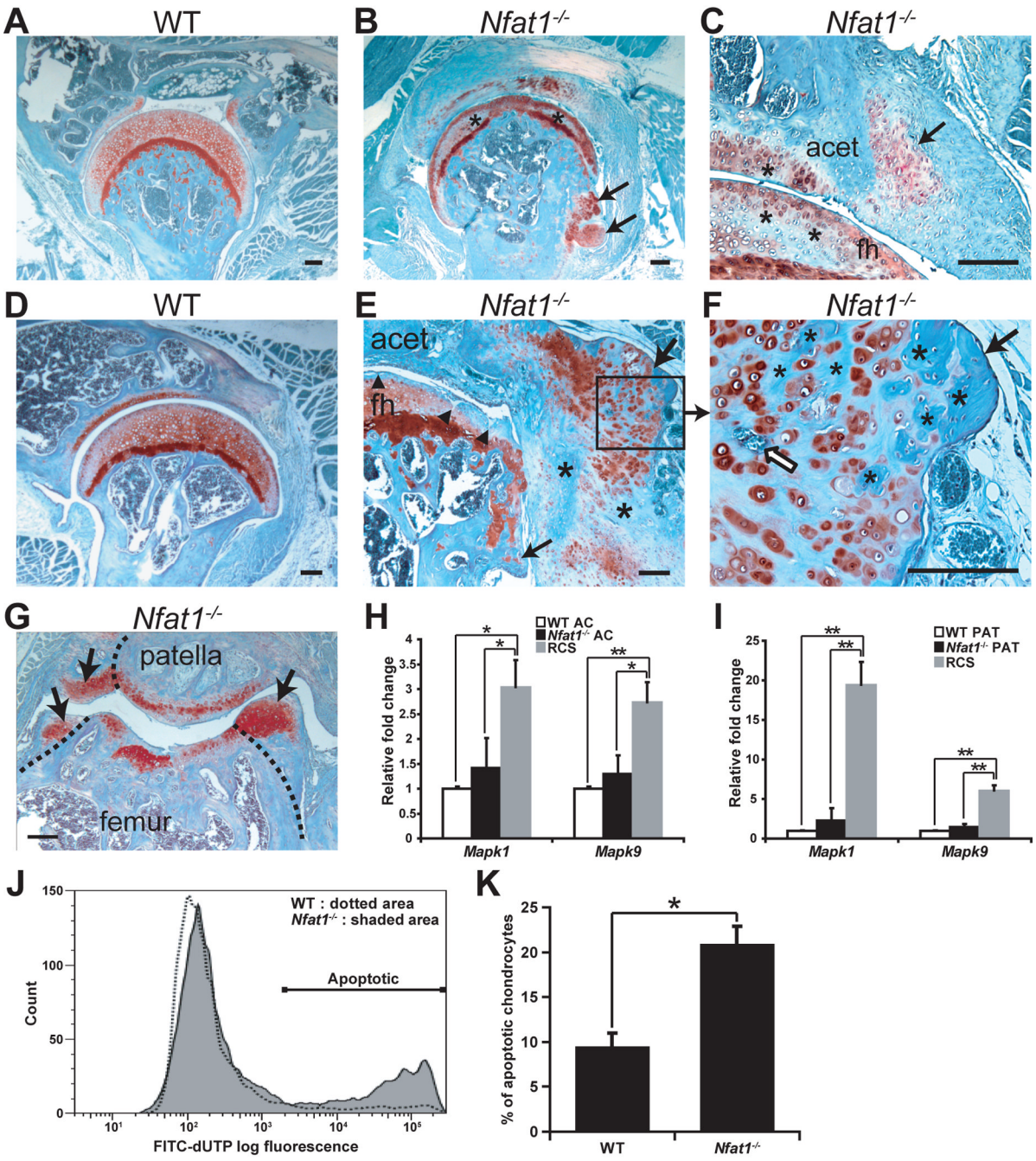

Figure 2.

Formation of chondro-osteophytes and apoptosis of articular chondrocytes in *Nfat1*$^{-/-}$ joints. All photomicrographs are representative of at least 5 *Nfat1*$^{-/-}$ or WT mice per gender at each time point. Safranin-O and fast green staining and counterstained with hematoxylin. Scale bar = 200 μm. (**A**) A 3-month-old female WT hip shows normal joint structure and articular surface with diffuse safranin-O staining (red) for proteoglycans throughout the articular cartilage. (**B,C**) Loss of safranin-O staining (*) with focal chondrocyte proliferation is observed in the upper-mid zones of articular cartilage of both femoral head and acetabulum in 3-month-old female *Nfat1*$^{-/-}$ mice, which is a feature of early (grade 1) OA [1]. Chondrocyte differentiation and chondrophytes have begun to appear at the junction of

articular cartilage and synovium (arrows) of *Nfat1*$^{-/-}$ hip joints. acet, acetabulum; fh, femoral head. (**D**) A 12-month-old WT hip shows normal joint structure and articular cartilage. (**E,F**) A 12-month *Nfat1*$^{-/-}$ hip shows loss of proteoglycan staining in the upper zone of articular cartilage with surface discontinuity and/or fissuring (▲) and chondro-osteophyte formation (arrows). The process of endochondral ossification is seen in the chondro-osteophytes, including chondrocyte hypertrophy and vascular invasion (open arrow). Cartilage has been partially replaced by newly formed bone (*). Although the development of chondro-osteophytes is exuberant, malignant-looking cartilage or bone cells with large single or multiple hyperchromatic nuclei and large nucleoli are not seen in periarticular chondro-osteophytes. (**G**) A 9-month *Nfat1*$^{-/-}$ patellar-femoral joint demonstrates articular cartilage degradation and the formation of chondro-osteophytes appearing as newly formed articular surfaces (arrows). Dotted lines indicate the surfaces of the original articular cartilage/bone. (**H,I**) qPCR analyses show no significant differences in expression levels of *Mapk1* and *Mapk9* between *Nfat1*$^{-/-}$ and WT articular cartilage cells (AC) or periarticular tissue cells (PAT), while their expression was significantly higher in positive control rat chondrosarcoma cells (RCS). According to the $2^{-\Delta\Delta C_T}$ method [23], the expression level of each WT group has been normalized to “one”. n = 3 pooled RNA samples, each prepared from the articular cartilage of 6–8 femoral heads or periarticular tissues of 3–4 joints. * $P < 0.05$; ** $P < 0.01$. (**J**) Flow cytometric analyses demonstrate substantially more apoptotic cells in *Nfat1*$^{-/-}$ chondrocytes than in WT chondrocytes isolated from 4-month-old femoral head articular cartilage. Overlays of flow cytometric analyses were made using FlowJo software (Tree Star). (**K**) Quantitative flow cytometric analyses indicate that significantly more apoptotic cells were detected in *Nfat1*$^{-/-}$ articular chondrocytes than in WT articular chondrocytes. $P < 0.05$.

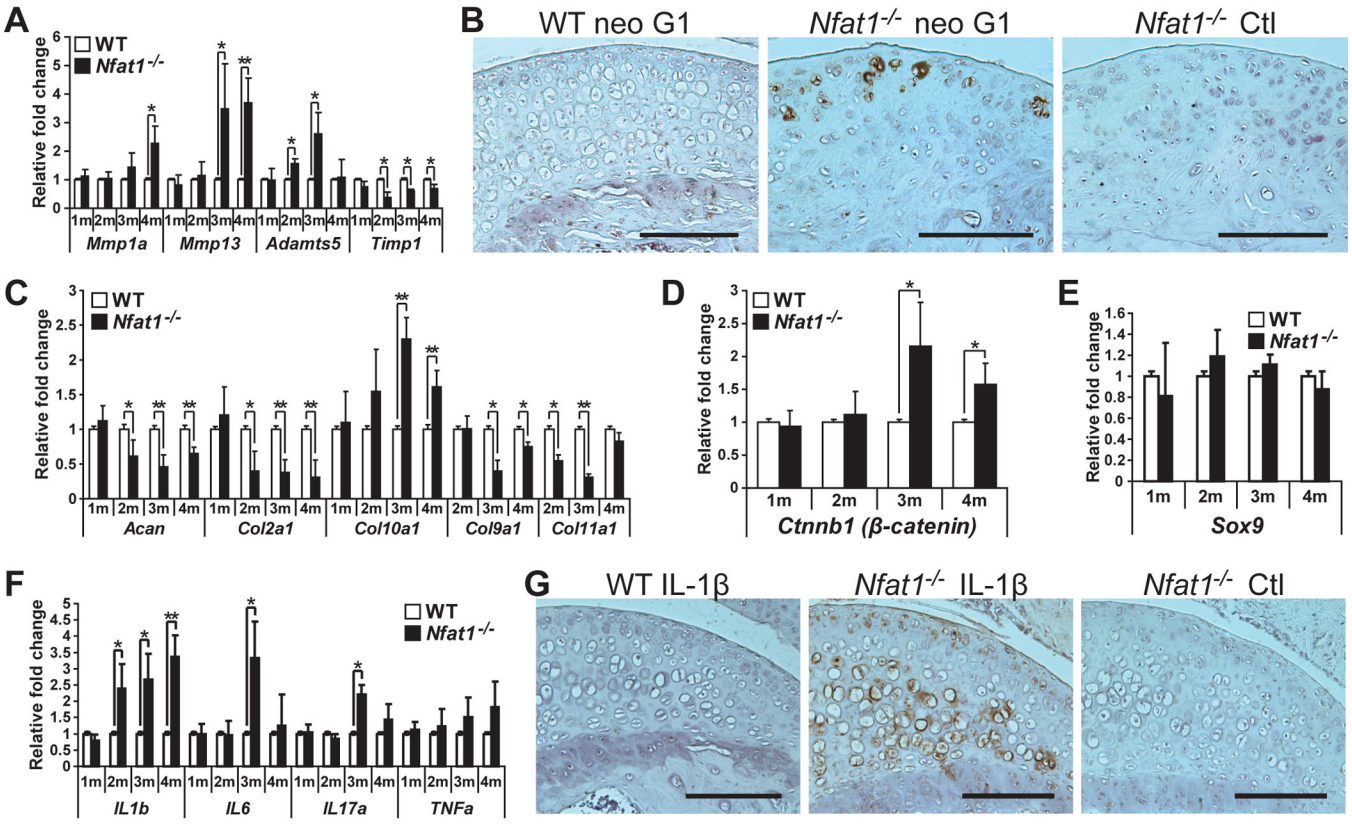

Figure 3.

Loss of Nfat1 leads to an imbalance between catabolic and anabolic activities of articular chondrocytes favoring catabolism. (**A**) qPCR analyses of genes of interest at 1–4 months (1–4m) demonstrate up-regulated expression of *Mmp1a, Mmp13, and Adamts5* and reduced expression of *Timp1* in femoral head articular cartilage of female *Nfat1*$^{-/-}$ mice compared to age-matched female WT mice. n = 3 pooled RNA samples, each prepared from the articular cartilage of 6–8 femoral heads; * $P < 0.05$; ** $P < 0.01$ for all qPCR analyses in Figure 3. (**B**) Immunohistochemical staining using an antibody (1:50) against human (cross-reacts with mouse) aggrecan neo G1 (Affinity BioReagents, PA1-1746), which detects the degraded aggrecan product, shows that staining of degraded aggrecan (brown areas) was substantially more intense around cells in the upper zone of 3-month old female *Nfat1*$^{-/-}$ femoral head articular cartilage than age-matched WT mice. *Nfat1*$^{-/-}$ Ctl represents a negative control without using neo G1 primary antibody. Scale bar = 200 μm for (B) and (G). (**C–F**) qPCR analyses indicate temporal changes in expression levels of various genes of interest in *Nfat1*$^{-/-}$ articular cartilage at 1–4 months. n = 3 pooled RNA samples, each prepared from the articular cartilage of 6–8 femoral heads. (**G**) Immunohistochemical analyses using a polyclonal antibody (1:50) against rat (cross-reacts with mouse) IL-1β (Santa Cruz, sc-1252) show substantially more intense expression of IL-1β (brown areas) in femoral head articular cartilage of 3-month-old *Nfat1*$^{-/-}$ mice compared to age-matched WT mice. *Nfat1*$^{-/-}$ Ctl represents a negative control using both IL-1β antibody and IL-1β blocking peptide (1:100) (Santa Cruz, sc-1252P) to validate the specificity of the immune reaction in *Nfat1*$^{-/-}$ articular cartilage.

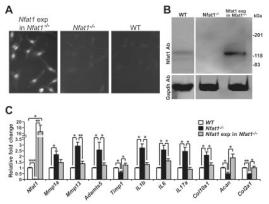

Figure 4.

Forced expression of Nfat1 rescues abnormal activities of 3-month-old *Nfat1*$^{-/-}$ articular chondrocytes. (**A**) Immunofluorescence using an antibody against hemagglutinin (HA) tags shows positive expression of Nfat1 protein in the nuclei of articular chondrocytes after lentiviral DNA transfection of constitutively active (CA) *Nfat1* plasmid with HA tags from Addgene (*Nfat1* exp in *Nfat1*$^{-/-}$), but not in control *Nfat1*$^{-/-}$ or WT articular chondrocytes in which HA tags are not present. Cultured cells for immunostaining were fixed with cold methanol for 15 minutes and incubated with the anti-HA-fluorescein high affinity (3F10) antibody (Roche, Cat.1988506) at a concentration of 5μg/ml in PBS for 1 hour at 22°C. After washing three times with PBS, the cells were observed and photographed using a Nikon (ECLIPSE TE300) fluorescence microscope equipped with a Spot RTKE camera. (**B**) Western blots using Nfat1 antibody (Nfat1 Ab) confirm the effectiveness of forced expression of CA-Nfat1 protein in cultured articular chondrocytes. Western blots using Gapdh antibody are presented as loading controls. (**C**) qPCR analyses indicate the expression levels of *Nfat1* and other genes of interest in cultured WT, *Nfat1*$^{-/-}$, and *Nfat1* exp in *Nfat1*$^{-/-}$ articular chondrocytes. n = 3 cultures. * $P < 0.05$; ** $P < 0.01$; *** $P < 0.001$.

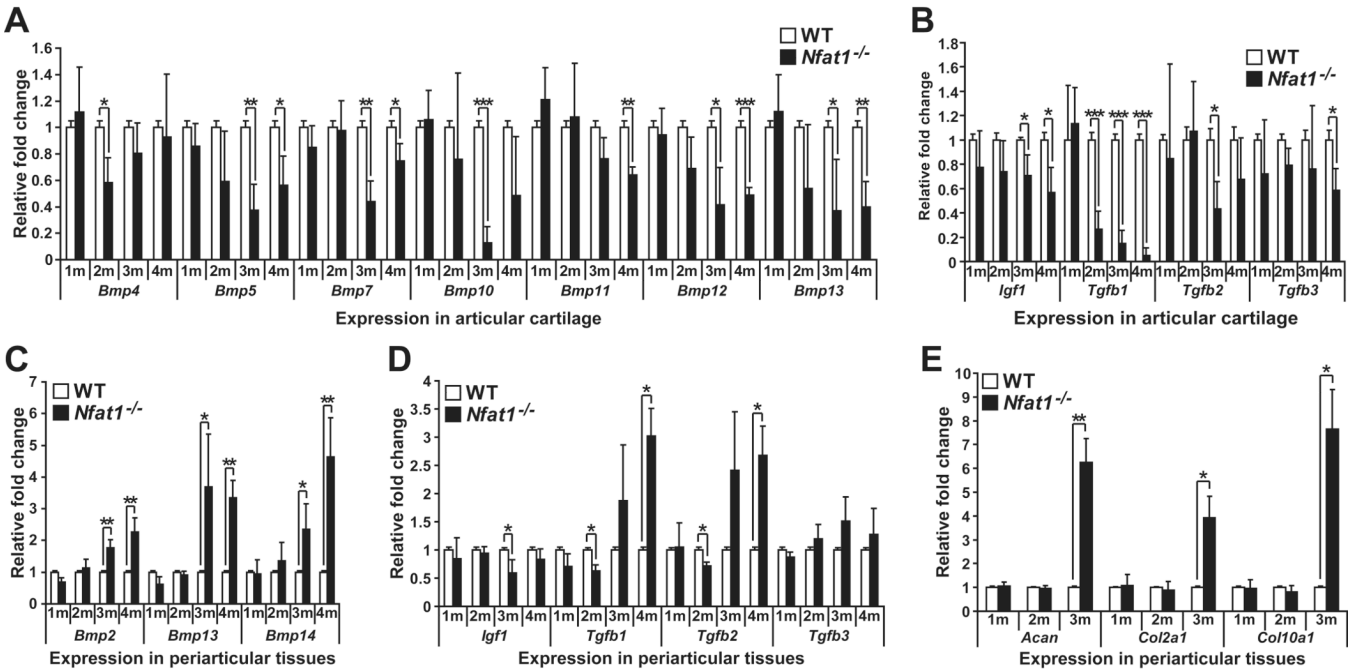

Figure 5.

Differential expression of specific growth factors between articular cartilage and periarticular tissues. (**A–E**) qPCR analyses of *Bmp2–15* (*Bmp* members without significant changes not shown), *Igf1*, *Tgfb1-3*, *Acan*, *Col2α1*, and *Col10α1* expression in femoral head articular cartilage and/or periarticular tissues of 1–4 months old (1–4m) $Nfat1^{-/-}$ and WT hip joints. n = 3 pooled RNA samples; each prepared from the articular cartilage of 6–8 femoral heads or periarticular tissues of 3–4 hip joints. * $P < 0.05$; ** $P < 0.01$; *** $P < 0.001$.

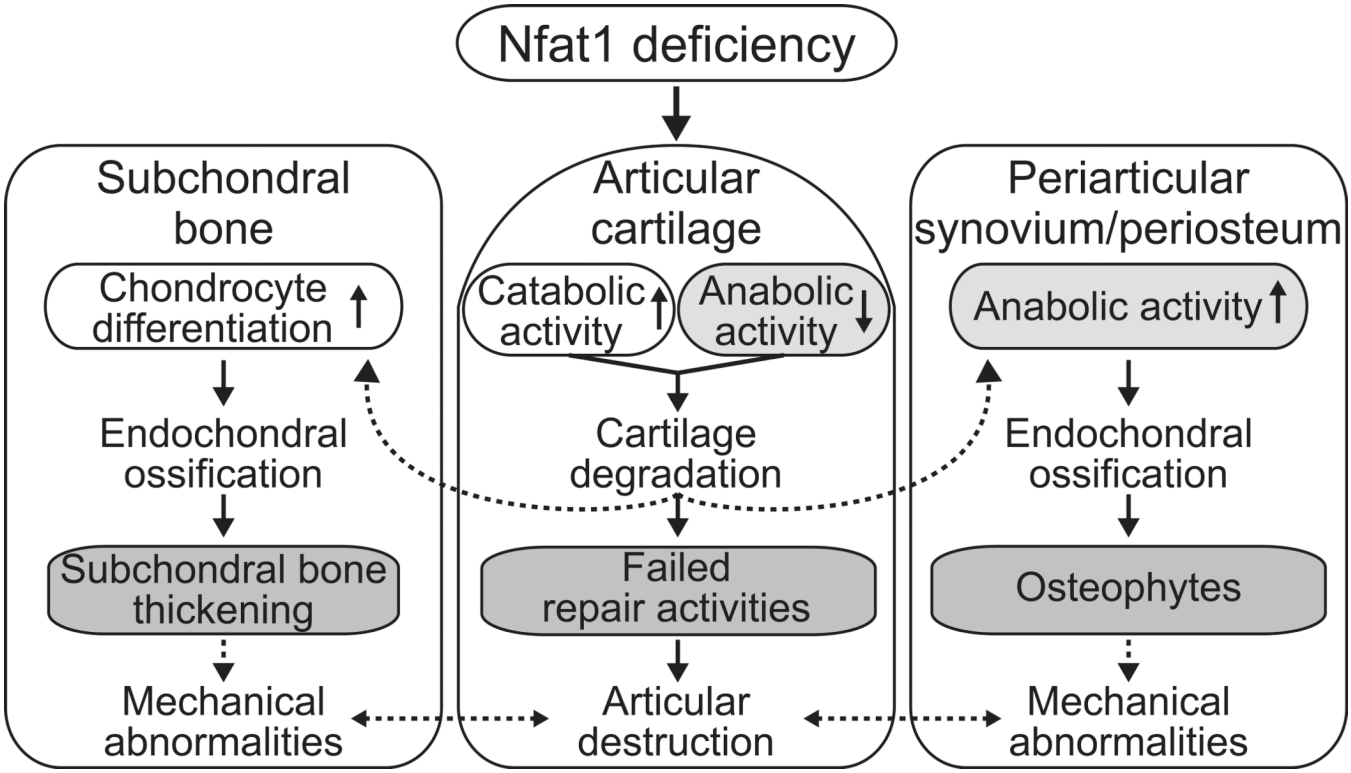

Figure 6.

A diagram showing possible mechanisms underlying Nfat1 deficiency-induced OA. Arrows with solid lines indicate mechanistic observations from this study. Arrows with dotted lines indicate proposed mechanisms described in previous publications [3,4,6,36,37]. Nfat1 deficiency initiates OA-like changes due to dysfunction of adult articular chondrocytes, leading to articular cartilage degradation and repair activities in and around articular cartilage. Periarticular osteophytes and thickened subchondral bone may cause abnormal mechanical loads on the joints and exacerbate the progression of OA, which supports the concept that OA is not exclusively a disorder of articular cartilage [4,6,36–38].